



Evaluating silica gel supported titanium dioxide for use as a photocatalyst
by Michael Owen Hardiman

A thesis submitted in partial fulfillment of the requirements for the degree of Master of Science in
Chemical Engineering
Montana State University
© Copyright by Michael Owen Hardiman (2001)

Abstract:

With increasing attention given to the clean up of polluted waters, new technologies need to be developed to offer safer, cheaper methods than those currently employed. Most current systems employ oxidizing agents which are costly, consumed in the process and often hazardous to work with. The use of titanium dioxide as a photocatalyst offers a safe alternative to current technologies and has been proven to degrade a wide number of contaminants. The majority of recent work in photocatalysis uses titanium dioxide slurry type reactors and separation is required to reclaim the catalyst. This will limit the applicability of this method due to the added separation expense. Supporting titanium dioxide for use in a packed bed configuration represents a viable alternative. Experiments were developed for the evaluation of supported titanium dioxide as a photocatalyst. Silica gel was chosen as a support material due to its unique properties regarding UV transmission, surface area and adsorptive capability for water and organics. The support materials were optimized for light transmission properties with respect to manufacturer, grade and size fraction. Coating methods were developed, and four continuous flow, annular reactors were designed to evaluate the supported photocatalysts. Through light measurements and kinetic experiments, four supported catalysts were evaluated in the four reactors for their ability to degrade formic acid. The degradation rates observed with the supported catalysts were found to have a strong dependence on catalyst loading and support material, but nonetheless outperformed slurry catalysts under identical conditions.

EVALUATING SILICA GEL SUPPORTED TITANIUM
DIOXIDE FOR USE AS A PHOTOCATALYST

by

Michael Owen Hardiman

A thesis submitted in partial fulfillment
of the requirements for the degree

of

Master of Science

in

Chemical Engineering

MONTANA STATE UNIVERSITY
Bozeman, Montana

December 2001

N 378
H 2149

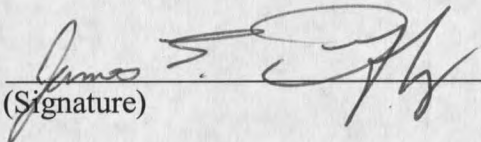
APPROVAL

of a thesis submitted by

Michael Owen Hardiman

This thesis has been read by each member of the thesis committee and has been found to be satisfactory regarding content, English usage, format, citations, bibliographic style, and consistency, and is ready for submission to the College of Graduate Studies.

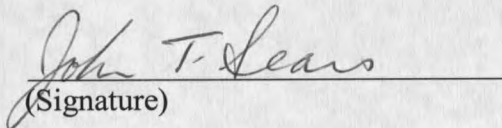
Dr. James Duffy


(Signature)

01-10-02
(Date)

Approved for the Department of Chemical Engineering

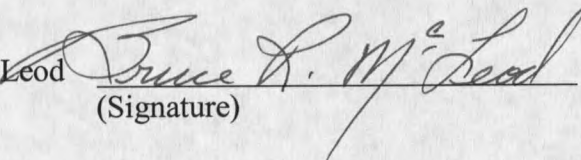
Dr. John Sears


(Signature)

01-10-02
(Date)

Approved for the College of Graduate Studies

Dr. Bruce McLeod


(Signature)

1-14-01
(Date)

STATEMENT OF PERMISSION TO USE

In presenting this thesis in partial fulfillment of the requirements for a master's degree at Montana State University, I agree that the Library shall make it available to borrowers under the rules of the library.

If I have indicated my intentions to copyright this thesis by including a copyright notice page, copying is allowable only for scholarly purposes, consistent with "fair use" as prescribed in the U.S. Copyright Law. Requests for permission for extended quotation from or reproduction of this thesis in whole or in part may be granted only by the copyright holder.

Signature

A handwritten signature in black ink, appearing to be "M. D. R.", written over a horizontal line.

Date

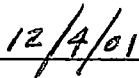
A handwritten date "12/4/01" in black ink, written over a horizontal line.

TABLE OF CONTENTS

1. INTRODUCTION AND BACKGROUND.....	1
Photocatalysis and Photocatalysts.....	3
Titanium Dioxide.....	5
Titania Surface.....	5
Mechanisms for Heterogeneous Photocatalysis using TiO_2	8
Catalyst Supports.....	11
Silica Gel.....	15
Photoreactors.....	16
Radiant Flux.....	18
Statement of Objectives.....	20
2. EXPERIMENTAL METHODS AND MATERIALS.....	22
Catalyst Supports.....	22
Light Penetration Tests.....	23
P25 TiO_2 Catalysts.....	25
TiO_2 Assay.....	26
Annular Reactors.....	26
Reaction Runs.....	29
Slurry Runs.....	30
Sample Analysis.....	31
3. RESULTS AND DISCUSSION.....	32
Choosing the Support Material.....	32
Light Penetration Through Annular Spaces.....	35
Coatings.....	36
Formic Acid Runs.....	37
Packed Bed Annular Reactor Runs.....	41
Slurry Runs.....	46
Data Analysis.....	49
Volume Correction.....	49
Normalization to Rate of Energy Absorbed.....	52
SEM.....	58
Conclusion.....	60
Future Work.....	62

TABLE OF CONTENTS - CONTINUED

REFERENCES CITED.....	63
APPENDICES.....	65
APPENDIX A.....	66
Formic Acid Runs Data.....	67
APPENDIX B.....	74
Spectrophotometric Method for the Determination of TiO ₂ Loading.....	75

LIST OF TABLES

Table	Page
1. Support Materials Used According to Size Fraction and Manufacturer.....	22
2. BET Data of the Silica Gels Used.....	23
3. Annular Reactor Dimensions.....	27
4. Five Consecutive Runs in 2.0" Reactor with 0.4 Weight Percent P25 on Grade 58.....	40
5. Summary of Supported and Suspended Observed Rates.....	48
6. Volume Corrected Rate Constants for the Various Catalysts.....	51
7. System Specific Extinction Coefficients.....	54
8. Summary of Intensity Normalized Rate Constants for the Various Catalysts.....	55
9. Comparison of Spectrophotometric and ICP-AS Methods.....	76

LIST OF FIGURES

Figure	Page
1. Charge Separation in a Semiconductor Particle Upon Excitation with Light.....	4
2. Surface Hydroxyl Groups on Titania.....	6
3. Photodegradation Rate Dependence on Radiant Flux.....	19
4. Acrylic Box Used in Support Material Light Penetration Tests.....	24
5. Light Intensity Measurements in Packed Annular Reactors.....	25
6. Annular Photoreactor.....	28
7. Schematic of Experimental Photoreactor Setup.....	29
8. Light Transmission Through Grade 58 Silica Gel and Borosilicate Glass Beads.....	32
9. Light Penetration Through Different Brands of 12-18 Mesh Silica.....	33
10. Light Penetration Through Various Size Fraction of Grade 58 Silica Gel.....	34
11. Comparison of Light Penetration Through Coated and Uncoated Silica.....	35
12. Light Penetration Through Annular Reactors Packed with Coated and Uncoated Silica.....	36
13. 2.00" Reactor Packed with 0.4 Weight Percent P25 on Grade 58 Silica.....	39
14. 2.0" Reactor Packed with 0.4 Weight Percent P25 on Grade 58 Silica at Varying Flow Rates.....	40
15. Observed Rate Versus Mass TiO_2 in Annular Reactors Packed with 0.4 Weight Percent P25 on Grade 58 Silica.....	41

LIST OF FIGURES - CONTINUED

Figure	Page
16. Observed Rate Versus Mass TiO_2 in Annular Reactors Packed with 0.04 Weight Percent P25 on Grade 58 Silica.....	42
17. Comparison of Grade 58 and Grade 55 Silica Gels.....	43
18. Light Penetration Tests with Uncoated 12-18 Mesh Silica Gel.....	44
19. Comparison of Observed Rates Versus Mass of Titania for the Various Catalysts.....	45
20. Comparison of Observed Rates with Supported and Suspended P25 Titania.....	47
21. Experimental Photoreactor System.....	50
22. Light Measurements for Intensity Balance on Photoreactors.....	53
23. Linearization of Equation 32 with Experimental Data to Give b Terms.....	54
24. Radial Dependence of k_{IC}	58
25. SEM of Silica Gel Particles.....	59

ABSTRACT

With increasing attention given to the clean up of polluted waters, new technologies need to be developed to offer safer, cheaper methods than those currently employed. Most current systems employ oxidizing agents which are costly, consumed in the process and often hazardous to work with. The use of titanium dioxide as a photocatalyst offers a safe alternative to current technologies and has been proven to degrade a wide number of contaminants. The majority of recent work in photocatalysis uses titanium dioxide slurry type reactors and separation is required to reclaim the catalyst. This will limit the applicability of this method due to the added separation expense. Supporting titanium dioxide for use in a packed bed configuration represents a viable alternative. Experiments were developed for the evaluation of supported titanium dioxide as a photocatalyst. Silica gel was chosen as a support material due to its unique properties regarding UV transmission, surface area and adsorptive capability for water and organics. The support materials were optimized for light transmission properties with respect to manufacturer, grade and size fraction. Coating methods were developed, and four continuous flow, annular reactors were designed to evaluate the supported photocatalysts. Through light measurements and kinetic experiments, four supported catalysts were evaluated in the four reactors for their ability to degrade formic acid. The degradation rates observed with the supported catalysts were found to have a strong dependence on catalyst loading and support material, but nonetheless outperformed slurry catalysts under identical conditions.

CHAPTER 1

INTRODUCTION AND BACKGROUND

This past century has seen a rapid increase in pollutants in our environment. Toxic pollutants in the soil, air and water are widespread. Continual human contact with toxins and the steady degradation of the environment is a growing concern on national and international agendas. The sources of these contaminants are extensive, ranging from (but not limited to) the chemical/petroleum industries, textiles, pulp and paper milling to increases in modern agriculture practices.

A considerable amount of research is currently being directed towards improving methods of contaminant treatment. Current processes in use such as air stripping or activated carbon adsorption offer only a phase change of the contaminant, likely requiring further treatment. Other methods, such as treatment with a strong oxidant (e.g. ozone or chlorine), generally offer less than complete removal of organic contaminants while consuming large quantities oxidants. Relatively new to the arena are methods collectively termed advanced oxidation processes (AOP's). These methods may be cheaper and offer better degradation than some of the above-mentioned methods. Examples of AOP's include direct UV photolysis of the contaminant, UV/ozone or UV/H₂O₂, and heterogeneous photocatalysis. The latter three of the these processes are of particular interest in that they have shown potential to kill bacteria as well as degrade organic compounds (1). Direct photolysis of an organic contaminant requires that it absorb the incident light and suffer degradation as a result. This is difficult to achieve

with most contaminants, especially at the low concentrations generally encountered in waste treatment. UV/ozone and UV/H₂O₂ have shown promise as effective treatment methods. When UV is used in conjunction with ozone or hydrogen peroxide, highly reactive hydroxyl ([•]OH) radicals are generated, which will non-selectively attack most organic compounds. While complete degradation is possible with these methods, large amounts of oxidant are consumed in the process. On the contrary, in heterogeneous photocatalysis reactive radicals (thought to be primarily [•]OH radicals) are generated *in situ* from air, oxygen or water (2) without the need for costlier and more hazardous oxidizers. In heterogeneous photocatalysis, a solid photocatalyst (usually an n-type semiconductor such as TiO₂, ZnO, or CdS) is illuminated with UV-visible light creating a reduction-oxidation (redox) environment (to be described in more detail later) that has been shown to be capable (3) of degrading a wide variety of organic contaminants. Other features that make heterogeneous photocatalysis attractive is that it generally uses low cost, non-toxic catalysts, can often be operated at ambient conditions and is capable of absorbing a wider portion of the UV spectrum efficiently as compared to other UV methods (2). In addition to air, water and wastewater treatment, heterogeneous photocatalysis has been used for a wide range of reactions including: mild organic oxidations, dehydrogenation, hydrogen transfer, O₂¹⁸-O₂¹⁶ and deuterium-alkane isotopic exchange, and metal deposition (4). Heterogeneous photocatalysis has been confirmed by numerous researchers to be effective for the total oxidation of organic water contaminants (5).

Photocatalysis and Photocatalysts

Though there is currently some dispute as to a proper definition of photocatalysis, a general definition is the "acceleration of a photoreaction by the presence of a catalyst"

(3). For the purpose of water treatment, heterogeneous photocatalysis can be loosely defined as the illumination of a particulate with UV-visible light of suitable energy to initiate redox chemistries (1) while the catalyst itself undergoes no overall change.

Semiconductors have largely been employed for use as photocatalysts because of their electronic structure, light absorption properties, charge transport characteristics, and excited state lifetimes (3). A detailed description of semiconductor materials is beyond the scope of this thesis and only some of the properties applicable to photocatalysis will be addressed. For a more complete treatment see Reference 6.

A semiconductor is characterized by a filled valence band and an empty conduction band. For a semiconductor material to be used as a photocatalyst, an excited state must be induced in the material by the absorption of light. Upon excitation by the absorption of a photon of sufficient energy, charge separation takes place as an electron (e^-) is promoted from the valence band to the conduction band. The absence of an electron in the valence band (or a positive charge) is known as a hole (h^+). The act of excitation by light is determined by the band gap, or the energy gap, between the valence and the conduction band energy levels. For promotion of an electron to occur, the photon energy must exceed the energy of the band gap.

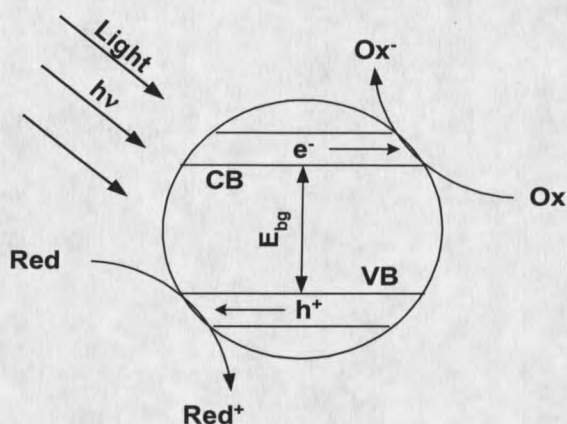


Figure 1. Charge separation in a semiconductor particle upon excitation with light ($h\nu > E_{bg}$). Ox and Red are oxidant (electron acceptor) and reductant (electron donor) respectively.

The existence of the band gap prevents rapid recombination (or deactivation of the excited state) of the electron-hole pairs (3). In the excited state, the electron and hole pairs will either recombine or diffuse to the surface of the semiconductor where they can participate in charge transfer reactions, though certain conditions must exist at the surface for this to occur. From Gratzel (3), "For semiconductor particles dispersed in a gaseous, liquid, or solid medium, the charge transfer can take place only in the presence of an electroactive species acting as electron donor or acceptor. Thus an interfacial redox reaction is required to produce the electric field within the particle". Species on the surface of semiconductors act as traps for the electrons and holes and prevent their recombination, allowing charge transfer to take place. For heterogeneous photocatalysis in the treatment of water, the electron donors and acceptors are mainly in the form of adsorbed oxygen and water molecules or surface bound hydroxyls (this to be treated in greater detail later).

Titanium Dioxide

In the area of water and wastewater treatment, the principal focus has been on the use of titanium dioxide or titania (TiO_2) as a photocatalyst. Mills and Le Hunte (7) proposed the following list of criteria in choosing a semiconductor for use as a photocatalyst:

1. Photoactive.
2. Able to utilize visible and/or near UV light.
3. Biologically and chemically inert.
4. Photostable (i.e. not liable to photoanodic corrosion for example).
5. Inexpensive.

Titania meets these criteria well and has been shown to exhibit a high photoactivity towards a wide range of compounds (7, 8). TiO_2 requires light less than 390 nm to be photoactive and has been shown to be capable of using sunlight to degrade organic pollutants (3). Approximately 4-6 % of the available sunlight (the amount of sunlight in the 300-390 nm wavelength region) has been demonstrated to initiate the photoactivity of titania (6).

Titania surface

In an aqueous environment, the surface of titania will be covered with hydroxyl groups. The extent of this coverage will depend on crystal phase and preparation conditions. The point of zero charge (PZC) of TiO_2 used in photocatalysis is in the pH range of 6-7 (3), with the surface positively charged in acidic environments. Titania is known to exist in three different crystal phases: anatase, rutile, and brookite.

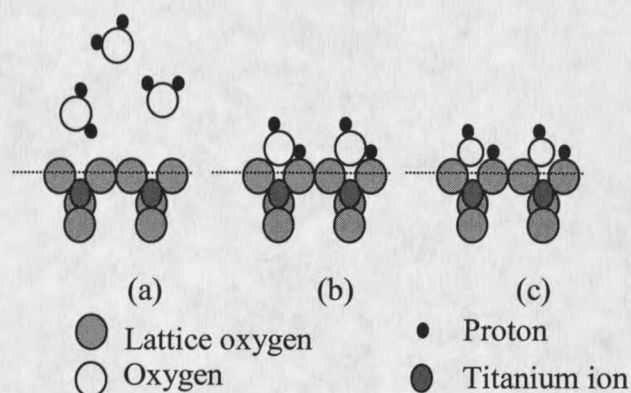


Figure 2. Surface hydroxyl groups on titania (17). (a) hydroxyl free surface; (b) physical adsorption of water; (c) dissociation of water, giving two distinct OH⁻ groups.

The annealing conditions will determine the crystal structure. Amorphous TiO₂ has been shown to exhibit low photoactivity (9), possibly due to decreased charge carrier mobility more easily attainable in definite crystal structures (10). Brookite is of no commercial significance and not used in photocatalysis. Of the remaining two forms, anatase has demonstrated the most photoactivity towards the degradation of organic compounds (3). Fox et al. (11) proposed that the lower photoactivity of rutile TiO₂ was due to its higher electron-hole recombination rate and its lowered capacity to adsorb oxygen, though Sclafani (11) found the activity of rutile to be influenced by its preparation conditions. Despite recent findings indicating that rutile TiO₂ may exhibit greater photoactivity towards certain compounds, particularly for the oxidation of CN⁻ (8), anatase is still the more practical form for widespread environmental applications. Anatase is thermodynamically less stable than rutile, though it is kinetically favored at temperatures < 600 °C (3). Optimizing the performance of titania with regards to annealing temperature has been the subject of several recent papers (8). Aside from the crystal

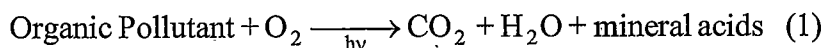
structure, the annealing conditions can control the morphology, specific surface area and surface density of OH groups (7). Hoffmann et al. (8) found the rates of 4-chlorophenol degradation to increase as the anatase form was calcined progressively from 100 to 400 °C and to decrease with TiO₂ calcined at 500 °C and above. Tanaka et al. (6) reported the degradation of several compounds to be dependent upon annealing conditions while independent for others. They also reported that TCE degradation rates increased for annealing temperatures up to 500 °C, and in some cases up to 700 °C, but decreased above those temperatures. Tsai et al. (11) found the photoactivity of laboratory produced rutile TiO₂ to decrease with calcination temperature and correlated it to the amount of OH groups on the surface. The general consensus seems to indicate that the photoactivity of titania decreases as the annealing temperature approaches the temperature of the rutile phase change (~600 °C). Moreover the higher annealing temperatures relieve the TiO₂ surface of OH groups essential to photoactivity. The increased photoactivity of anatase therefore is thought to arise from a larger surface area and a higher surface density of active sites for adsorption and photocatalysis.

The majority of titania used in photocatalysis comes in three forms: a pre-made TiO₂ powder, TiO₂ particles precipitated from a sol-gel, and TiO₂ produced by chemical vapor deposition (CVD) of titanium chlorides (TiCl₃ and TiCl₄) on some support. The pre-made powders come in a controlled crystal structure and particle size (generally anatase on the nm to μm scale). Starting from a titanium salt, sol-gel techniques can produce titania from a sequential process of hydrolysis, polycondensation and drying of a colloidal suspension (12). Sol-gels can generally produce small (~10nm) amorphous and

crystalline TiO₂ particles, where crystal structure and particle size is a function of preparation conditions (pre-cursor sol, calcining conditions, pH, etc.). Titania from CVD is obtained by exposing a surface to titanium chlorides and water vapor at high temperatures (~200–500 °C), where the water vapor will substitute for the chlorides. Ultrafine thin films of titania on silicon and quartz substrates have been reported using CVD techniques (13). Obviously, there are numerous variations on sol-gel and CVD techniques that can affect particle growth and crystal structure. The chemistry involved is beyond the scope of this paper. A good treatment of colloidal semiconductors can be found in Reference 3.

Mechanism for heterogeneous photocatalysis using TiO₂

Certain features of photoinduced reactions involving semiconductor catalysts have previously been mentioned. Some will be repeated here for clarity in the specific case of heterogeneous photocatalysis involving TiO₂ and the degradation of aqueous organic contaminants. The overall process of the photodegradation of organics with TiO₂ can be summarized as follows

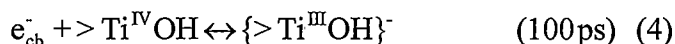
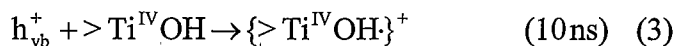


Though the exact mechanism for the heterogeneous photodegradation of aqueous organics is not completely understood, it is known that the primary process involves electron-hole pair formation followed by interfacial electron transfer to form surface bound oxidants (7). Based on laser flash photolysis measurements, Hoffman et al. (8) proposed the following mechanisms, with their characteristic times, for surface reactions on illuminated TiO₂.

Charge carrier generation



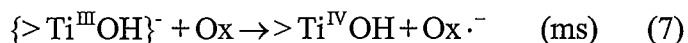
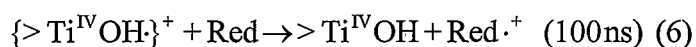
Charge carrier trapping



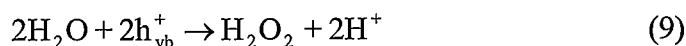
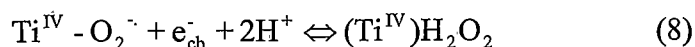
Charge carrier recombination



Interfacial charge transfer



The overall success of a photocatalytic reaction is dependent on the competition between charge carrier trapping and recombination (Equations 3-4 & 5). The above mechanism assumes all oxidation of organics occurs via surface bound hydroxyl $\{> \text{Ti}^{\text{IV}}\text{OH}\}^+$ attack, though oxidation may occur with between free radicals and liquid phase organics as well (14). Also not mentioned in this scheme is the formation of hydrogen peroxide from dioxygen reduction with conduction band electrons and possibly from valance band hole oxidation of water (15). These two pathways can be represented as follows (14, 15):



It has been noted that H_2O_2 may contribute to the degradation of pollutants by acting as a direct electron acceptor or as a further source of hydroxyl radicals due to homolytic splitting (15).

Though it is assumed that hydroxyl radicals are the primary oxidant in TiO_2 systems, it is not known if oxidation principally occurs via surface bound or free radicals.

Turchi and Ollis (14), in an effort to determine the role of hydroxyl radicals in TiO₂ photocatalysis, proposed four possible mechanisms for hydroxyl radical attack.

1. Reaction occurring while both organic and hydroxyl are adsorbed.
2. A non-bound radical reacts with a bound organic.
3. An adsorbed radical reacts with a free organic.
4. Reaction occurs between free radical and organic.

Four kinetic models were derived for the above, relating degradation of a single component by way of hydroxyl attack. All resembled Langmuir-Hinshelwood (L-H) rate forms.

$$r_i = \frac{k_{\text{obs}} \kappa C_i}{1 + \kappa C_i} \quad (10)$$

It was found that k_{obs} was the same for each of the four cases in the degradation of 14 organic compounds, suggesting that it is a function only of catalyst properties and reaction conditions. Further differentiating between reactions of adsorbed and free radical to suggest a dominant form was not possible. Estimates of diffusion/reaction rates with free OH radicals and liquid phase organics suggest that even at low organic concentration, free radicals would not diffuse very far into solution before reacting ($\sim 10^{-8}$ – 10^{-6} m). Based on these estimates, they found it plausible that OH is present as a mobile radical. It is likely that some combination of these mechanisms is present during heterogeneous photocatalysis.

In most photocatalytic systems, oxygen acts as an electron acceptor. The current view is that electrons are consumed by dioxygen to produce the superoxide radical anion,

O_2^- (1), with subsequent electron transfer reactions leading to the formation of H_2O_2 . Supporting this view is work by Serpone et al. that noted no degradation occurs in the absence of oxygen (3). Control batch experiments by our group in which aqueous phenol suspensions of TiO_2 were sparged with nitrogen also found no degradation to take place. Serpone has observed superoxide radicals on the surface of illuminated TiO_2 in the presence of oxygen (1). Hoffmann et al. (15), using ^{18}O isotopic labeling with a ZnO photocatalyst noted that all of the photochemically produced H_2O_2 is from dioxygen. They also reported that hydrogen peroxide was not detected in the absence of oxygen.

Catalyst Supports

Much of the work in liquid phase photocatalysis using TiO_2 has been conducted in slurry type reactors using very fine titania particles (e.g. Degussa P25 TiO_2 : ~30nm in diameter). These types of reactors have several advantages. In perfectly mixed reactors, there will be no segregation of phases and with fine particles (nm scale), the entire external surface can be illuminated during the reaction (12). Also these reactors have a large ratio of surface area of TiO_2 per unit volume of the reactor, limiting mass transfer effects (16). In modeling these systems, they can be (at least to a first approximation) treated as "pseudo-homogenous" and amenable to simple laws such as the Beer-Lambert law (12). Overall though, the utility of these reactors is limited, as recovery of the catalyst downstream of the reactor is difficult.

Fixing the catalyst on a support of some sort is the alternative. Certain tradeoffs come with immobilizing the catalyst though. Degradation rates may be mass transfer

limited and the catalyst-photon interactions will be more limited. These limitations will be dependent on specific reactor/support configurations.

Pozzo et al. (13), in a recent review of research on supported TiO_2 for use in environmental photocatalysis, suggested the following attributes of a good photocatalyst support:

1. Transparent to UV radiation.
2. Favor strong surface chemical-physical bonding with the TiO_2 particles without negatively affecting their reactivity.
3. Offer a high specific surface area.
4. Have good adsorption capability for the organic compounds to be degraded.
5. Be in a physical configuration which favors the ultimate liquid-solid phase separation.
6. Allow reactor designs that facilitate the mass transfer processes.
7. Be chemically inert.

Early work on immobilized photocatalysts involved coating the inner glass walls in an annular type reactor (17) or the inner wall of a glass coil wrapped around a circular light source (18, 19). Degradation rates for these flow-by type reactors were found to suffer from boundary layer mass transfer limitations, as only a portion of substrate will be in contact with the catalyst at any given time (20).

In the last decade, much attention has been directed towards immobilizing TiO_2 on various substrates including; particles (silica, alumina, zeolites, activated carbon, glass

beads etc.), quartz optical fibers, glass fiber or wool (12, 13). Various forms of reactor design have been employed, including packed, fluidized and floating bed reactors. Based on the current interest here, the following discussion will be restricted to particle supports applicable for packed bed applications.

Recent research has shown that supports can alter photoactivity in several ways. For example, Xu and Langford (21) comparing two different zeolites, silica gel, and alumina, related increased adsorption of organics on the support to increased photoactivity. Concerning zeolites, they proposed increased photoactivities could be related to the rigid framework of the surface, where reactive radicals, such as $\cdot\text{OH}$ and O_2^- , could be stabilized on the surface where they can be efficiently reached by organic molecules. Xu et al. (9), in a comparative study of preparation methods for coating silica gel with sol based TiO_2 , also related increased photoactivity to increased adsorption of organics. Rates reported for supported catalysts were considerably higher than those obtained with bare catalysts. In these experiments degradation rates were found to be higher with smaller silica gel particles. They reported that smaller silica particles resulted in the formation of smaller TiO_2 particles on the surface. It was suggested that smaller silica particles cause the TiO_2 to be more dispersed on the surface (possibly affecting crystallinity) and more efficient as a photocatalyst.

Surface characterization of supported catalysts is important in that the crystal structure of titania on the support can be determined and related to its photocatalytic behavior. Also, determining how TiO_2 is adhering to the support will allow predictions of the durability of a specific catalyst under reaction conditions. Xu et al. (9) found that

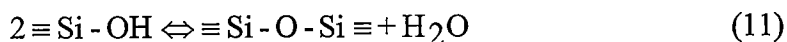
supporting TiO_2 on silica restricts crystal formation even after calcining. They reported a film of amorphous TiO_2 to exist on the surface, limiting photoactivity. Xu and Langford (21) found that at low coverage, TiO_2 on zeolite is amorphous, only forming well-defined anatase crystals at higher coverage. Structure determination of supported titania is made difficult at lower loadings commonly encountered in environmental photocatalysis (generally less than 1 wt. %). Differentiating between X-rays of the catalyst/support surface in X-ray diffraction (XRD) analysis is difficult at such low loadings, making the results suspect. Similarly, scanning electron microscopy (SEM) of supported surfaces reveals little about the true nature of the catalyst-support interactions. Islands of what appears to be titania have been reported to appear on supported surfaces (12), suggesting a random, highly dispersed coating. Xu and Langford (21) suggest that these particles may form on a thin coat of titania after monolayer capacity has been exceeded. Verifying this would require slicing a coated particle and viewing it from the side. This would allow determination of the thickness of a titania layer if it formed as a uniform coat. The small size of most support materials (μm – mm scale) makes this difficult and slicing would likely damage the coating.

TiO_2 adherence to the support is an essential aspect in supported photocatalysts, yet many papers on the subject neglect it entirely (9, 16, 18, 21). If supports readily lose their titania (or a substantial portion of it) to the fluid phase, the reason for its use is compromised. Adherence is generally evaluated at reaction conditions. Analysis of the catalyst after subjecting it to flows high enough to eliminate mass transfer concerns will allow quantification of adherence. Bideau et al. (12) in a comparison of supports, titania,

and coating methods, found pre-made powder (P25 TiO₂) coatings to adhere better to silica gel than coatings using a sol-gel process (loss of 52% for sol compared to 21% for P25 powder). Zhang et al. (22), using powder (Aldrich TiO₂) coated silica gels, reported no noticeable attrition of TiO₂ after 1 hour under flow and no decrease in photoactivity after a 20-day run. Though coating methods used by the Bideau and Zhang groups were similar for powder coatings, widely varying results were obtained. These results can be somewhat misleading in that reactor configurations differed. The setup used by Zhang et al. was a packed tubular reactor and that used by Bideau et al. was a CSTR with the catalyst placed on the bottom. It would be natural to assume that supported catalyst in a packed bed would be subjected to greater stress and yet they reported no loss of catalyst. Such results could be explained by the fact that different silica gels, titania powders, and calcining conditions will produce different coatings, one performing well and one not. This makes direct comparisons between different researchers difficult.

Silica Gel

In this study, silica gel (SiO₂) was chosen as a photocatalyst support for its ability to meet several of the above mentioned criteria. It transmits UV light well, has high specific surface area (~100-1000 m²/g) and is chemically inert. The surface of silica gel is covered by hydroxyl and siloxane groups. Hydroxyl groups can be arranged on the surface in various ways with one or two hydroxyls bound to a single Si atom (23). Siloxane groups are formed by a partially reversible dehydroxylation between hydroxyl groups at about 500 K (3). This can be represented as follows



In an aqueous environment, silica gel is capable of taking up water and organics by means of physical adsorption (23), with the amount dependent on temperature, surface density of hydroxyl groups, pH, and specific surface area. The point of zero charge (PZC) for most silica gels is at a pH of about 2 (3). Above this pH, the surface will be negatively charged, limiting its adsorptive capabilities for negatively charged ions. Aside from the above support criteria, silica gels also exhibit high thermal stability and high mechanical strength (24).

Coating a support with sols or pre-made powders generally involves mechanical mixing of a liquid suspension of titania and the support material followed by calcining and washing. For the case of silica gel, titania bonding likely occurs at surface hydroxyls with the attraction being Van der Waals forces (24). The degree of dispersion of titania on silica will therefore be dependent on the surface density of hydroxyls on silica (and also titania particle size) (24). This surface density of hydroxyls will change with calcining temperature. With other coating methods such as CVD there is evidence of Ti-O-Si linkages at the surface, which will alter the electronic properties of the catalyst (24).

Photoreactors

Photodegradation rates will be dependent on reactor design, as the geometry will determine light distribution. Numerous reactor designs utilizing sunlight and artificial light have been employed in photocatalytic work and are described elsewhere (4, 8, 17, 22, 25, 26). By far, the configuration most used in bench scale operations is the lamp in tube annular reactor. This reactor represents a simple and very efficient configuration utilizing artificial light (27) and is probably the best type for commercial applications.

Reliable design equations for annular photoreactors using a solid catalyst have yet to be developed. These equations are complicated by the coupled mass and energy (photon) balances that would have to be performed and the uncertainty of certain parameters (namely light absorption and scattering coefficients) (28). Theoretically, mass/energy balances would have to be performed for each wavelength when using polychromatic light (27). Pseudo-homogenous approximations for absorption and scattering coefficients have been determined for some slurry reactors but are lacking for supported catalysts. In theory, these parameters would be different for each catalyst/support combination and have to be determined on case-by-case basis. Due to the nature of these systems, absorption and scattering coefficients for larger, supported catalysts are generally unattainable and built into the few models that exist as assumptions (27, 28). This subjects the coefficients to a high degree of uncertainty.

Since lamps come in finite sizes, the majority of bench reactors are scaled to utilize a light of certain dimensions, often with no other criteria. Obviously, reactor materials should be chosen that transmit light of the desired wavelengths. Parameters that can be easily ascertained are the light intensity as a function of distance and light penetration through packed beds of certain catalysts. Using this knowledge, the outer diameter of the reactor should be fixed such that a percentage of the entering photons can reach the outer most catalyst. Despite such measures, a photon gradient will exist with radial distance from the lamp in an annular reactor. If it is substantial, a resultant concentration gradient may develop where faster degradation occurs closer to the light.

Lamps should be chosen that emit light below the threshold wavelength (i.e. of enough energy to overcome the bandgap energy of the catalyst) and ideally operate in the regime where first order dependence on intensity holds (see below). It should also be verified that the liquid phase reactants do not absorb light in order to conserve light for the catalyst.

Radiant Flux

The rate of a photocatalyzed reaction will be proportional to the flow of photons reaching the catalyst. Using titania for aqueous degradation of organics, many researchers have found the relationship to resemble Equation 13.

$$\text{Rate} \propto (\text{Intensity})^n \quad (12)$$

The power n has been found to vary from a first order dependence at low intensities to a square root dependence at high intensities (8). Hoffmann et al. (15) explained this on a kinetic basis using ZnO (an n-type semiconductor like TiO_2) in the photoproduction of hydrogen peroxide. Assuming that the reduction of oxygen by surface trapped electrons is the rate-limiting step, they proposed the following equation to calculate the concentration of photoexcited electrons.

$$\frac{d[e_{cb}^-]}{dt} = I - k_a[e_{cb}^-][h_{vb}^+] - k_b[Zn^{II}OH_2^+][e_{cb}^-] + k_{-b}[Zn^I OH_2] \quad (13)$$

Where I is the light intensity generating electron/hole pairs, $k_a[e_{cb}^-][h_{vb}^+]$ represents the

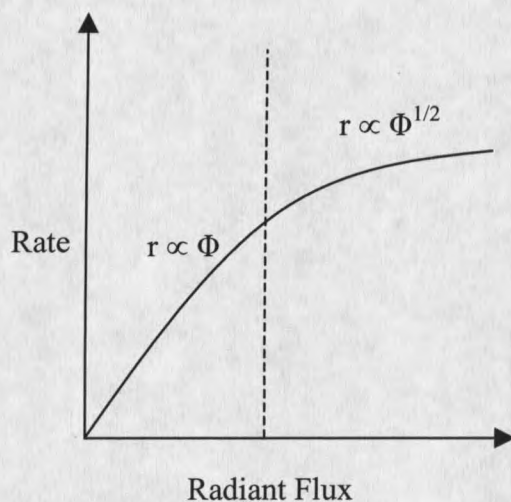


Figure 3. Photodegradation rate dependence on radiant flux.

rate of electron/hole recombination, and the remaining terms represent the rate of reversible surface trapping of a conduction band electron. Using a steady state approximation for the concentration of electrons and assuming that $[e_{cb}^-] = [h_{vb}^+]$, solving for intensity gives

$$I = k_b[Zn^{II}OH_2^+][e_{cb}^-] - k_{-b}[Zn^I OH_2] + k_a[e_{cb}^-]^2 \quad (14)$$

At high light intensities (i.e. high electron concentrations) the third term in Equation 14 is much larger than the other two and simplifies to

$$[e_{cb}^-] = \left(\frac{I}{k_a} \right)^{\frac{1}{2}} \quad (15)$$

Whereas, at low intensities the first two terms in Equation 14 will dominate, giving first order dependence on light intensity.

$$[e_{cb}^-] = \frac{I + k_{-b}[Zn^I OH_2]}{k_b[Zn^{II} OH_2]} \quad (16)$$

This assumes that the production rate of electrons by the reverse of the electron trapping reaction is small compared to the rate of production by photon absorption. Thus, at higher light intensities second order recombination will dominate over first order trapping mechanisms.

Furthering this, Hoffmann et al. (15) determined quantum yields for the rate of adsorbed oxygen reduction with surface trapped electrons (assuming this to be the rate limiting step). Quantum yields can be defined as the rate of reaction to the rate of photon absorption (15). It was found that the quantum yield will be proportional to intensity to the negative one half power at high light intensity and independent of intensity at low light intensity.

Statement of Objectives

The work presented here represents a preliminary attempt in the development of supported TiO₂ catalysts for use in photoreactors. Through the use of multiple reactors, light measurements and kinetic studies it was desired to evaluate the effect of catalyst loading on light penetration and degradation rates of formic acid. The focus of this study breaks down as follows:

- Optimization of support materials.
- Light penetration through uncoated supports.
- Light penetration through coated support materials.

- Reactor design for flow through packed bed system (titanium dioxide supported on silica gel).
- Design a kinetic experimental system.
- Determine catalyst loading and reactor dimensions that are most effective in degrading formic acid.

CHAPTER 2

EXPERIMENTAL METHODS AND MATERIALS

Catalysts Supports

Several silica gels were examined for their light transmission properties. Unless noted, the silica gels were crushed and screened to the indicated size fractions. Listed below in Table 1 are the various support materials used in this project. Glass beads were used as a comparison.

Table 1. Support materials used according to size fraction and manufacturer.

Support	Mesh (U.S. Standard)	Size (mm)	Manufacturer
Silica Gel Grade 55	12 - 18	1.68 - 1.00	Grace Davison
Silica Gel Grade 646*	35 - 60	0.50 - 0.25	Grace Davison
Silica Gel Grade 41	12 - 18	1.68 - 1.00	Grace Davison
Silica Gel CS - 0470	12 - 18	1.68 - 1.00	PQ Corporation
Silica Gel Grade 58	4 - 7	4.76 - 2.83	Grace Davison
	7 - 12	2.83 - 1.68	
	12 - 18	1.68 - 1.00	
	18 - 25	1.00 - 0.71	
	25 - 35	0.71 - 0.50	
	35 - 60	0.50 - 0.25	
Borosilicate Glass Beads	18	1.00	Chem Glass
Glasperlen Glass Beads	18	1.00	Braun

* Used as purchased

Following crushing and screening, the gels were washed several times with Milli-Q water to remove fines and dried at 110°C. BET-Nitrogen adsorption (Micromeritics Model ASAP 2000) was used to characterize surface area and pore size distribution of the

coated and uncoated silica gels. Subsequent to size fractionation, support materials to be coated were fired in a muffle furnace with a ramp rate of 3°C/min to 350°C and soaked for seven hours at that temperature. The reason for the heat treatment was to prepare the materials for firing following coating. If a material was to experience surface alterations during firing it would be preferable if it occurred prior to coating. During the heat treatment, the surface area of some silica gels would decrease up to 25%, probably the result of pore widening. The decrease in surface area of coated silica gels is likely due to both pore widening and pore blocking by the titania. Scanning electron microscopy of some coated and uncoated Grade 58 silica gel was performed with a JEOL Model 6100 SEM.

Table 2. BET data of the silica gels used.

Sample	BET surface area m ² /g	Avg. Pore Diam. Å
Gd.58-Not fired	270	161
Gd.58-Fired	236	195
Gd.58-0.4%TiO ₂ -P25	232	192
Gd.58-0.04%TiO ₂ -P25	224	197
Gd.41-Fired	707	23
Gd.41-0.4%TiO ₂ -P25	655	22

Light Penetration Tests

A box made of cast clear acrylic was constructed for tests of light penetration through packed beds of support materials. The acrylic transmitted nearly 100% of the UV light. The interior of the box was partitioned to allow for varying bed depths. On the back

of the adjustable portion of the box an International Light Super-Slim (model SSL001) UV probe was attached and used in conjunction with an International Light photometer (model 1400A).

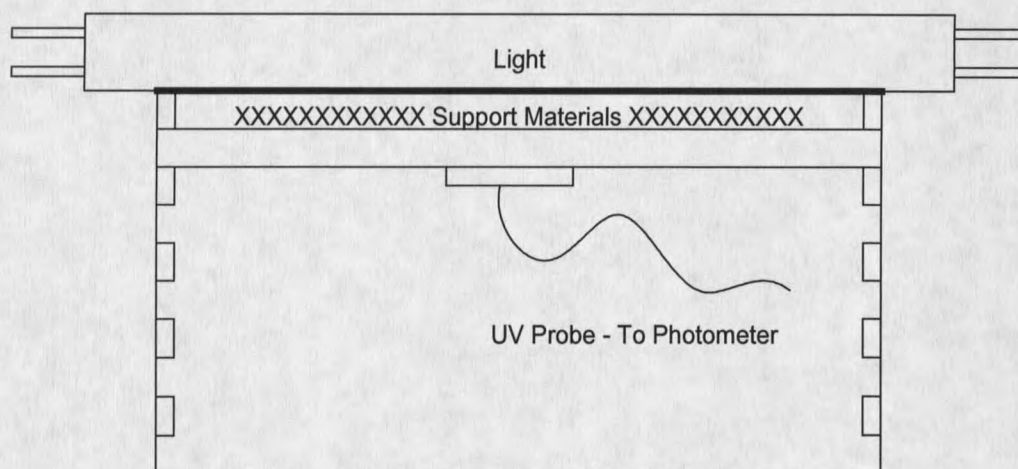


Figure 4. Acrylic box used in support material light penetration tests (top view).

The probe was factory calibrated to detect UV in the 250-400 nm range with a maximum at 375 nm. A 15-Watt black light was fixed in place and centered on the front of the box. Bed depths of 0.5, 1.0, 1.5, 2.5 and 3.5 cm were examined. Radiant flux readings, in mW/cm^2 , for the various packed beds were normalized with empty bed values.

In the annular photoreactors, light intensity readings were taken with the UV probe fixed at azimuth angle of ninety-degrees and in a direct line to the center of the light. Measurements were taken with the probe butting the surface of the inner and outer reactor tubes. As there was some variability in intensity readings with the packed reactors (particularly with the two smaller reactors as the annular space was just a few particle diameters), four readings were taken by rotating the reactor ninety-degrees around the axis. These four values were averaged. A slight correction was made to outer intensity

readings to account for the change in radial distance due to the tubing wall thickness as this tubing varied for the four reactors. Intensity readings taken on the outer surface of the inner tube (r_i) were denoted initial intensity, I_i , for each reactor.

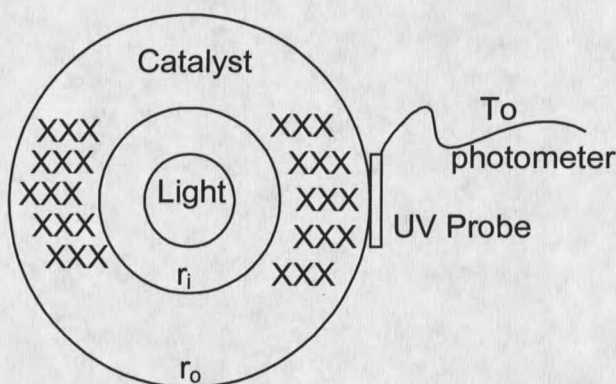


Figure 5. Light intensity measurements in packed annular reactors. Four readings taken at ninety-degree intervals around outer tube (end view).

P25 TiO₂ Catalysts

The P25 brand TiO₂ powder was a gift from the Degussa-Huls Corporation. As supplied in powder form, P25 TiO₂ particles are on the order of 30-60 nm in diameter. For coating silica gel, the desired amount of P25 was added to enough Milli-Q water to cover the silica. The suspension was then sonicated for 15 minutes using a Heat Systems-Ultrasonics sonicator (model W-380) to break up any agglomerates. Following sonication the suspension was added to the silica gel and mixed. Coated silica was dried at 60 °C for several days until all free liquid was evaporated, and then dried at 110 °C for one day to drive out any pore liquid. The coated silica was finally fired with the same conditions for the uncoated silica. These conditions were chosen based on catalyst preparation work performed at the University of Wisconsin-Madison Water Chemistry Department. The

fired catalysts were then washed and dried at 110 °C. With this method 40-50% of desired adherence was possible, the remainder dropping out of solution as a powder. Further refinement of P25 coatings was not attempted.

TiO₂ Assay

To determine the amount of titania adhering to the support material, a spectrophotometric method was adapted from Jackson et al. (29) (see Appendix B for details of this method). Briefly, the coated support was digested in a sulfuric acid/ammonium sulfate solution and the Ti(SO₄)₂ content was assayed by addition of H₂O₂, which forms a yellow colored complex with an absorption maximum at 410nm. The absorbance was linear with titanium complex concentration over the range employed. To determine the reliability of this method, some standards and samples were also analyzed with inductively coupled plasma atomic spectroscopy (Model ARL Accuris). The two methods correlated well (See Appendix B for data).

Annular Reactors

Four annular reactors of varying outer tube diameter were constructed. The top priority in material selection for these photoreactors was light transmission of the inner reactor wall between the light source and the photocatalyst. This wall must transmit light at the proper wavelength to irradiate the catalyst. For titania to be photoactive, the wavelength must be less than 390nm. The lights used in these experiments emitted near UV light between 300 – 400nm with a maximum at ~355nm. This emission spectrum allows the use of borosilicate glass, instead of more expensive quartz which is required

for medium and short wave UV applications. For all reactors, borosilicate glass was chosen as it transmits UV greater than 300 nm. The three criteria for material selection for reactor end pieces were; strength (as considerable compression had to be exerted to seal the reactor), workability, and inertness to the reacting fluid. Teflon (PTFE) fit these criteria well and was the chosen material for reactor end pieces and tubing. Silicone O-rings served as sealing gaskets between the glass tubes and Teflon end pieces.

Table3. Annular reactor dimensions.

Reactor Designation	Outer Tube Diameter (mm)	Annular Space (mm)	Bed Volume (mL)
2.00	50.80	3.20	64.90
2.25	57.15	6.35	135.70
2.50	63.50	9.53	216.70
2.75	69.85	12.70	327.20

The annular reactors were designed to utilize a 15 W black light 1 inch in diameter by 18 inches in length. The reactor was chosen to be 7 inches in length and use the center portion of the lamp, as light intensity decreases towards the ends of the lamp. The light intensity was approximately constant over this portion of the lamp. All four annular reactor configurations used an inner glass tube of 1.5 inches in diameter and had a bed length of 6.5 inches. Three ports for in flow and out flow were spaced at 120° in the annulus and the end pieces were staggered so as not to provide straight flow through the reactors. To further support the catalyst in the reactor and prevent large inlet void spaces due to flow, glass wool was placed at the top and bottom of the reactors.

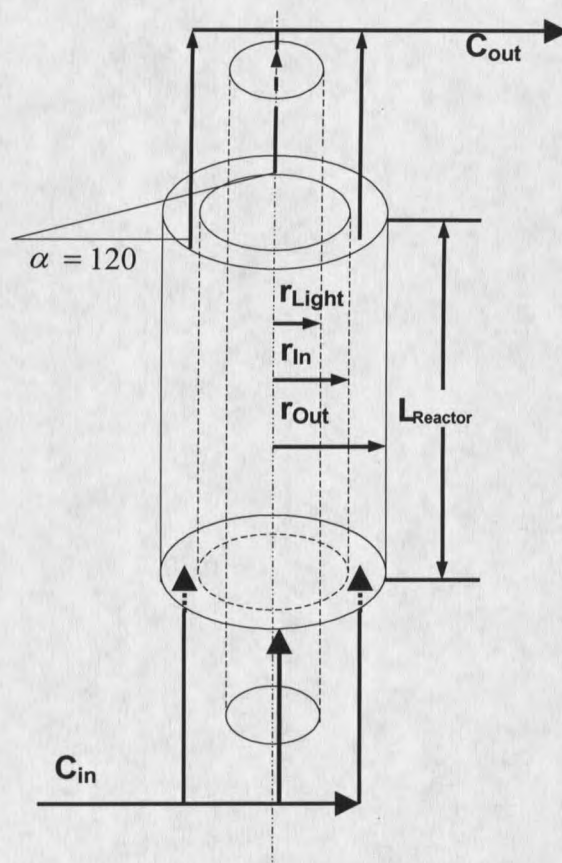


Figure 6. Annular photoreactor (end caps not shown).

The experimental setup was a continuous recycle system consisting of a reservoir bottle in line with a pump, sample valve and the reactor. Oxygen was supplied to the reservoir bottle through a sparging line during reaction runs. Stirring was accomplished with a magnetic stir plate and a Teflon coated stir bar. The lines to and from the reactor were manifolded with a four way connector to supply the three inlet and outlet ports. Once packed and assembled the reactor was vertically mounted to provide consistent flow.

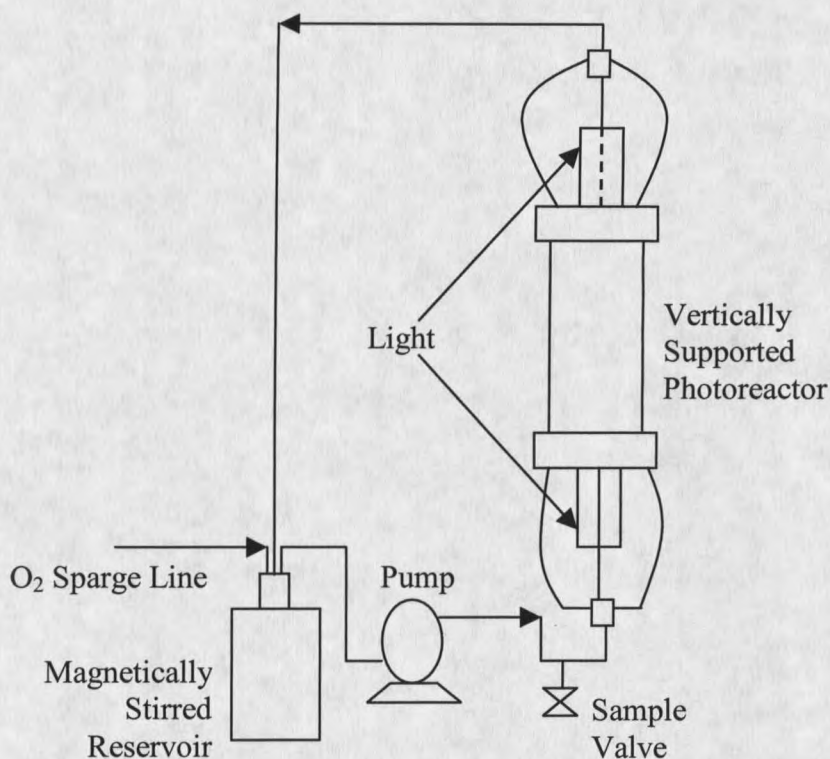


Figure 7. Schematic of experimental photoreactor setup.

Reaction Runs

Unless noted, all experiments were performed at a concentration of 100-PPM carbon (corresponding to 383-PPM formic acid). Prior to placing the reactor on recycle, 2 to 5 liters of the formic acid solution (dependent on reactor volume) was run through in single pass mode to establish adsorptive equilibrium. Following the single pass run, the light was turned off, the reactor drained of all free liquid and 1 L of 100-PPM C was set to run on continuous recycle. When the reactor was full of liquid, the lamp was turned back on marking time zero for the run. Reservoirs containing the formic acid solution were sparged with oxygen one hour prior to use and sparged continuously throughout the run while being stirred magnetically. A valve installed in line between the pump and the

reactor was used for sample withdrawal. Samples (approximately 1 mL) were taken starting at $t = 60$ min. and intermittently thereafter until run completion. Depending on catalyst loading, runs would last from four to eight hours, usually until it was estimated that at least 80% degradation had occurred. On average, eight to ten samples were taken per run. After completion of all experiments with a particular reactor, fluid was drained and the reactor was air dried. Catalyst removed from the reactor was further dried at $110\text{ }^{\circ}\text{C}$ and weighed. Assumptions made for this setup were as follows:

- Absorptive equilibrium was established after running solution through single pass.
- Solution was saturated with oxygen.
- Perfect mixing was present in the reservoir.
- Plug flow through reactors was present.

Slurry Runs

As a comparison, experiments using powdered TiO_2 slurries were also conducted in each of the four annular reactors. Procedures for the suspended runs were similar to those for the packed beds. A measured amount of P25 TiO_2 was added to the reservoir containing the formic acid solution to be degraded. To finely disperse the titania particles, the resultant slurry was sonicated for fifteen minutes. The P25 powder in the formic acid solution remained finely dispersed throughout the runs (no significant agglomeration or settling of particles was observed). Aluminum foil was wrapped around the reservoir bottle to prevent stray UV light from causing degradation in the reservoir. The bottle was sparged with oxygen for 1 hour prior to pumping and sparged continuously throughout

the run while under magnetic stirring. To rule out the disappearance of formic acid due to adsorption on the titania, samples were taken prior to powder addition and after the addition of TiO_2 and 1 hour of stirring and sparging. No statistically significant adsorption of formic acid was noted. The slurry was run through the reactor on continuous recycle using a peristaltic pump at flows corresponding to those of the packed bed runs. Sampling procedures were the same as mentioned above for the packed bed runs. Prior to analysis, samples were centrifuged for 6 minutes at 14000 rpm using a Fisher Scientific Micro 14 microcentrifuge.

Sample Analysis

Formic acid concentrations were determined using a Dohman Carbon (TOC) Analyzer (DC-80). Direct aqueous injections of 100 μL were possible and no refinement of samples was necessary. Repeatable results were obtained with an average percent standard deviation of less than 2 percent. All samples were refrigerated immediately and usually analyzed within 24 hours.

CHAPTER 3

RESULTS AND DISCUSSION

Choosing the Support Material

For preliminary evaluation of catalyst support materials, light penetration studies were conducted using the acrylic box described previously. As indicated in Figure 8, silica gel does not strongly absorb UV light and in comparison with borosilicate glass beads, it can be seen that the silica gel would be the better choice for a photocatalyst support.

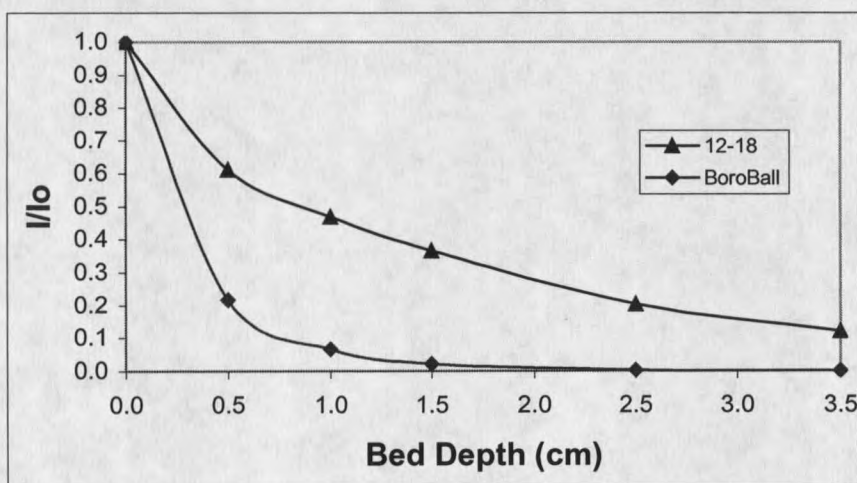


Figure 8. Light transmission through Grade 58 silica gel and borosilicate glass beads.

UV transmission through silica gel was found to be dependent on manufacturer and/or grade and size fraction. Light penetration tests were conducted to find the optimum grade and size fraction for the support material to be used in the photoreactors. Intensity values were normalized with empty bed values. Regarding size fraction for the support

materials, consideration was given to minimizing pressure drop, reducing loss due to entrainment under flow conditions, and working with reasonable bench scale annular spaces.

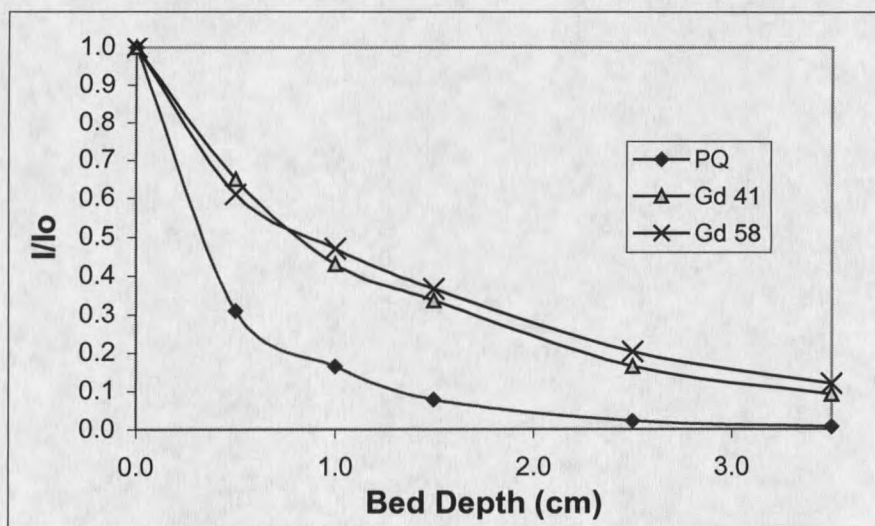


Figure 9. Light penetration through different brands of 12-18 mesh silica.

Based on the data shown in Figure 9, Grade 58 silica gel was chosen for further study. Though Grade 41 showed similar light transmittance to the Grade 58, it was found to burst on contact with water. BET analysis revealed it to be microporous with a surface area greater than $700 \text{ m}^2/\text{g}$. It is possible that a high heat of adsorption with water is the cause. This obviously makes it ill suited as a support in an aqueous environment.

To determine the most effective size fraction for use, Grade 58 (obtained in 4-7 mesh size from the distributor) was crushed and screened to five smaller fractions. As indicated in the Figure 10, approximately 50 to 75 percent of the light is absorbed in the first 10mm of packed bed with the chosen silica gels. It should be noted that light intensity readings at the 5 mm bed depth for the larger size fractions are highly dependent

on packing as this space is only 1-3 particle diameters. Based on the size fraction tests it was concluded that 12-18 mesh grade 58 silica gel would perform best as a photocatalyst support material.

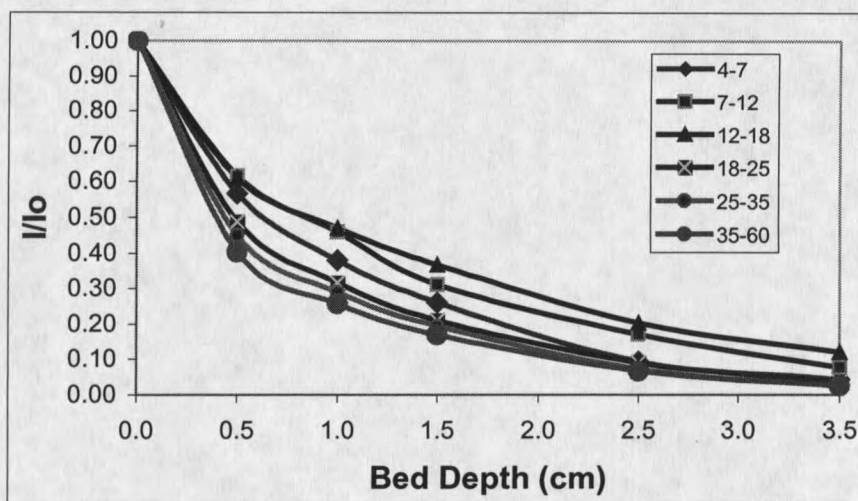


Figure 10. Light transmission through various size fraction of Grade 58 silica gel.

Referring to Figure 11, the effect of loading the silica gel with titania can be seen to be substantial. Light penetration tests through a 0.02 weight percent TiO_2 loading shows a marked decrease in light transmission within the first few millimeters of bed. Approximately a 70 percent difference in light transmission was observed between the unloaded and loaded catalyst at a bed depth of 1.0 cm.

These measurements served as a basis for the design of the photoreactors. Four annular reactors were designed with annular spaces ranging from 3.2 to 12.7mm. These were practical sizes for the reactors, considering the catalyst size, drop in light transmission and the available materials.

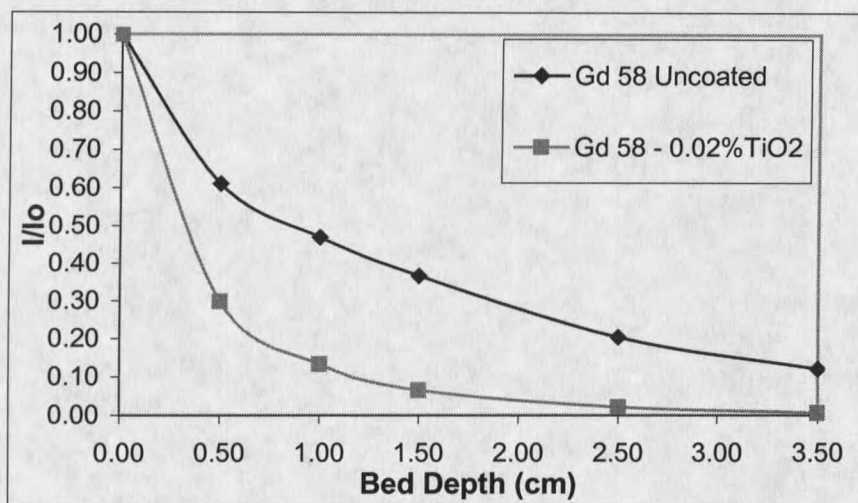


Figure 11. Comparison of light transmission through coated and uncoated silica.

Light Penetration Through Annular Spaces

Light penetration data taken in the acrylic box gave a general idea of the UV transmission properties of silica gels. It should be noted that the light penetration tests conducted in the acrylic box may be subject to some error due to the geometry of the box. There exists the possibility that light can exit the box in several different directions other than the direct line between the light and the probe. UV transmission through a cylindrical geometry is expected to differ from linear bed measurements in that the bed area increases with radial distance. In this configuration, light can be assumed to only exit through the outer glass of the reactor (the Teflon end caps will transmit light but this was determined to be negligible). After packing each reactor with coated and uncoated supports, intensity readings were taken at the outer surface of the four outer tubes. Referring to Figure 12, the first data points represent light readings on the outer surface

of the inner glass and the successive data points represent light readings on the outer surface of each of the four reactors.

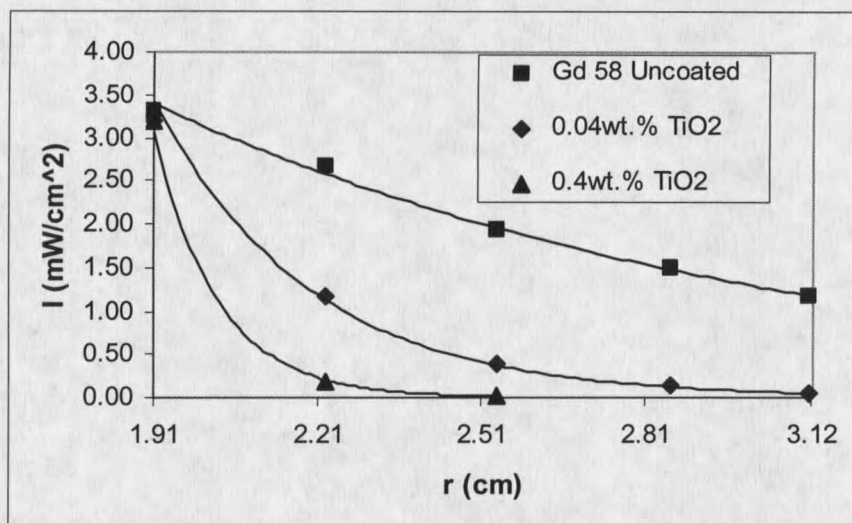


Figure 12. Light penetration through annular reactors packed with coated and uncoated silica.

Similar to linear bed measurements, the effect of loading silica gel with TiO₂ greatly affects light distribution through the annular reactors. Approximately 95 % of the incoming light is absorbed in the first three millimeters (the smallest reactor) of reactor space with a 0.4 weight percent TiO₂ loading.

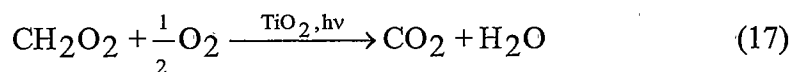
Coatings

From the light penetration tests, a 0.4 weight percent loading was determined to be the practical upper limit. At higher loadings, light would likely be undetectable outside even the smallest reactor. To test the adherence of titania to the silica, the 2.0" reactor was packed with a 0.4 percent loading and reaction conditions simulated for several hours. Following the run, the catalyst from the reactor was assayed at a 0.35 weight

percent loading. As this is within the variability of the analysis method, it is difficult to determine if there was an actual loss of titania. It is possible that unattached fines not removed during catalyst washing were fully removed under flow. Fines in this system would contribute little to the overall degradation rate, as they would not be under constant illumination.

Formic Acid Runs

Formic acid was chosen as the compound to test the photoactivity of the catalysts because it has a simple molecular structure, is easily photodegraded, is highly soluble in water, and there is limited possibility for intermediate radical formation (30). The photooxidation of formic acid can be represented as follows



Two blank runs were performed to confirm that the disappearance of formic acid occurred only in the presence of illuminated titania. To rule out photolysis of formic acid due to absorption of UV light and volatilization from the reservoir during sparging, a blank run was performed in an empty, illuminated annular reactor. Another run was conducted in an illuminated annular reactor packed with uncoated silica gel. This experiment was performed to rule out degradation of formic acid due to an interaction with the silica gel. There was no loss of formic acid in either blank run after several hours of illumination. It was also noted that formic acid, at the concentrations used, did not absorb UV light.

Numerous researchers involved in heterogeneous photocatalysis have found some form of the Langmuir-Hinshelwood rate expression to fit degradation data well (4,22,26).

$$r_i = \frac{k_{\text{obs}}\kappa C_i}{1 + \kappa C_i} \quad (18)$$

Where k_{obs} is the reaction rate constant, κ is the adsorption constant, and C_i is the concentration of substrate. In cases of high and low substrate concentration, apparent zero order and first order rates, respectively, have been observed. If the Langmuir-Hinshelwood rate expression accurately describes the kinetics, the second term in the denominator of Equation 18 would dominate at high substrate concentrations and cancel with the numerator giving:

$$r_i = k_{\text{obs}} \quad (19)$$

For the case of low substrate concentration, the 1 in the denominator of Equation 18 would dominate giving apparent first order rates.

$$r_i = k_{\text{obs}}\kappa C_i = k_{\text{app}}C_i \quad (20)$$

As indicated in Figure 13, initial runs using a 0.4 weight percent P25 loading on Grade 58 silica gel show that the degradation of formic acid follows apparent zero order kinetics at the higher concentrations used (100 PPM C). The linearity of concentration versus time data is seen to decline at concentrations below about 20 PPM C. This was confirmed in a run with a starting concentration of 15 PPM C where apparent first order degradation was observed. The observed kinetics are consistent with data presented by Kim et al. (35), which shows a transition between zero order and first order kinetics between 17.5 and 35 PPM formic acid. All subsequent runs used an initial concentration of 100 PPM C.

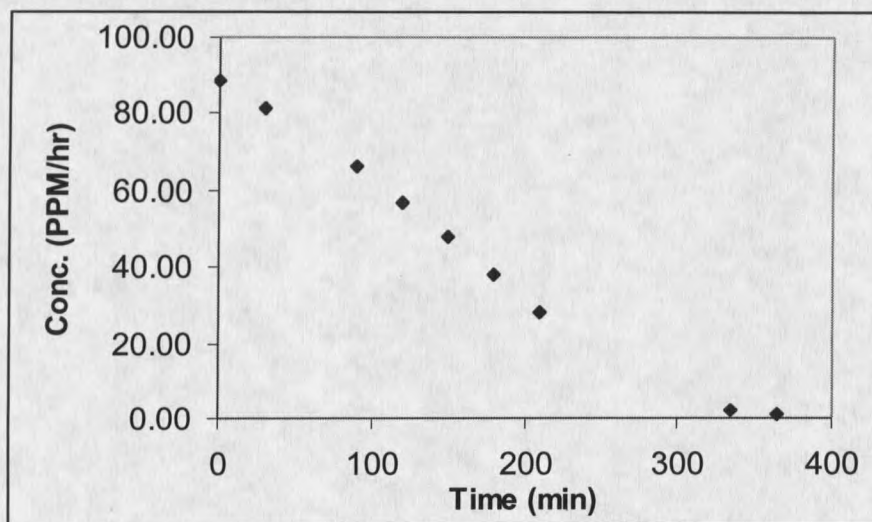


Figure 13. 2.00" Reactor packed with 0.4 weight percent P25 on Grade 58 silica.

It is known that reaction rates in packed bed configurations will have a dependence on flow as mass transfer limitations may exist below a threshold flow rate. To determine if there were mass transfer limitations in the annular systems, four runs were conducted at different flow rates to see if a drop in rate was observed. Starting at a flow of 150 mL/min (the highest possible with the pump and setup used) four runs were conducted, incrementally reducing the flow to 25 mL/min.

The observed rate remained constant for flows of 50, 100 and 150 mL/min with approximately a ten-percent drop for a flow of 25 mL/min (Figure 14). All subsequent runs were performed at flows between 100 and 150 mL/min.

As the assay test to determine the adherence of TiO_2 to the silica gel was inconclusive, further tests were conducted. The 2.0" reactor was packed with fresh

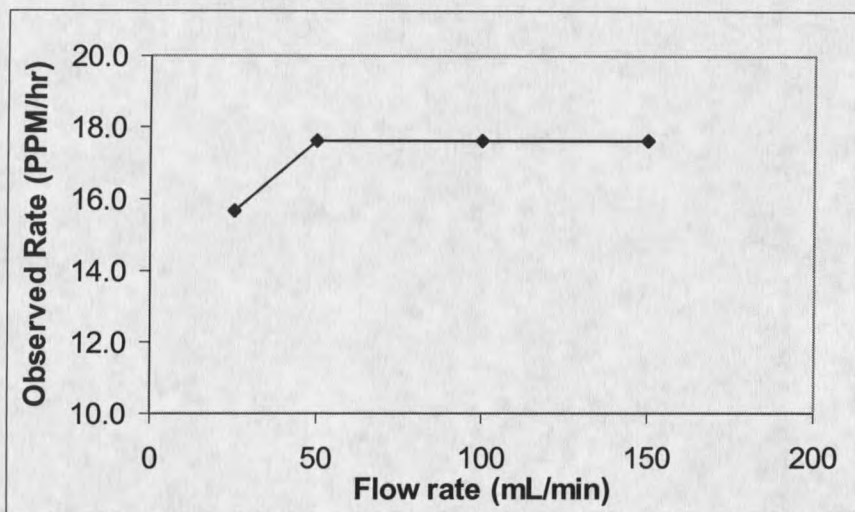


Figure 14. 2.0" reactor packed with 0.4 weight percent P25 on Grade 58 silica at varying flow rates.

catalyst and subjected to five consecutive runs at a flow rate of 100 mL/min to determine if the degradation rate decreased as a result of catalyst loss. After the fourth run, the reactor remained under flow for 90 hours before the fifth run. With approximately a three-percent variability in reaction rates, there does not appear to be a change in reaction rates due to erosion of titania.

Table 4. Five consecutive runs in 2.0" reactor with 0.4 weight percent P25 on Grade 58.

Run	Rate (PPM/hr)
1	16.8
2	17.4
3	18.2
4	17.2
5 (After 90 Hrs. under Flow)	17.4

Packed Bed Annular Reactor Runs

Several of the experiments with the supported catalysts in the four reactors were randomly performed twice to demonstrate repeatability with the setup and methods used. Rate data generated from the repeated runs was used to calculate an average standard deviation in rates of approximately 5 percent. Error bars in all subsequent figures showing rate data represent plus and minus one standard deviation.

As stated above, a 0.4 weight percent loading was taken as the upper limit of catalyst loading in the evaluation of the annular photoreactors. Using a 0.4 weight percent P25 loading on Grade 58 silica gel, identical runs were conducted in the four reactors.

Figure 15 depicts a run in each of the four annular reactors with increasing mass of TiO_2 corresponding to the increasing volume of the reactors. It can be seen that increasing the mass of TiO_2 had little or no effect. This was not unexpected as 95 % of the light was absorbed in the first 3.2mm of annular space at this loading and therefore, titania in the reactor past this point is not activated.

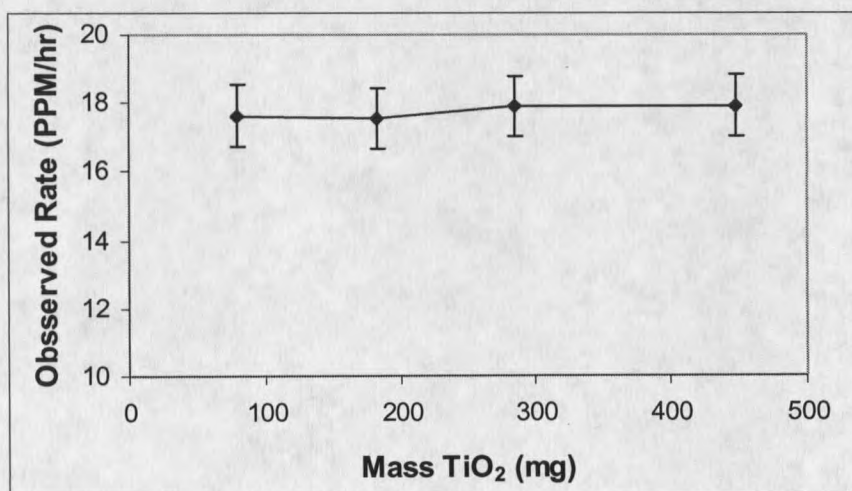


Figure 15. Observed rate versus mass TiO_2 in annular reactors packed with 0.4 weight percent P25 on Grade 58 silica.

In the next set of experiments, the TiO_2 loading was decreased an order of magnitude to 0.04 weight percent P25. It was desired to see more of a pronounced effect on rates with increasing reactor volume. The absorption of light was less severe at this loading and light was able to penetrate the packing in all reactors (i.e. light was detected at the outer surface of each reactor).

As indicated in Figure 16, the observed rate is seen to increase with mass of TiO_2 but appears to be leveling off with the largest two reactors. At this loading the light detected outside the largest reactor corresponded to absorption of 99 % of the incident light entering the reactor. Increasing the bed volume past this point would have little effect at this loading and the observed rates would likely have a maximum around 13-14 PPM/hr.

Based on the data presented, experiments were planned for titania loadings between 0.04 and 0.4 weight percent to better examine the effect of light distribution on rates. However, new silica gel had to be obtained at this point as the previous loadings

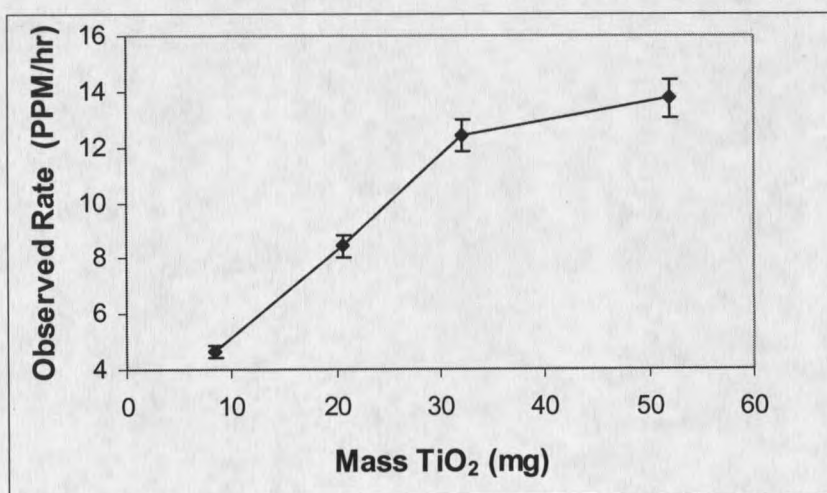


Figure 16. Observed rate versus mass TiO_2 in annular reactors packed with 0.04 weight percent P25 on Grade 58 silica.

used the remainder of the stock. Upon consulting the supplier (Aldrich Chemicals), it was discovered that the manufacturer had discontinued Grade 58 but was supplying the same gel in different size fractions as Grades 55 and 59 (both > 8 mesh). As indicated in Figure 17, a 0.1 weight percent P25 loading prepared with Grade 55 silica (12-18 mesh) did not give the results expected. A small increase in degradation rates was observed in the two smallest reactors with 0.1 weight percent P25 on Grade 55, but quickly leveled off to perform worse than the 0.04 weight percent P25 Grade 58 catalyst in the larger two reactors.

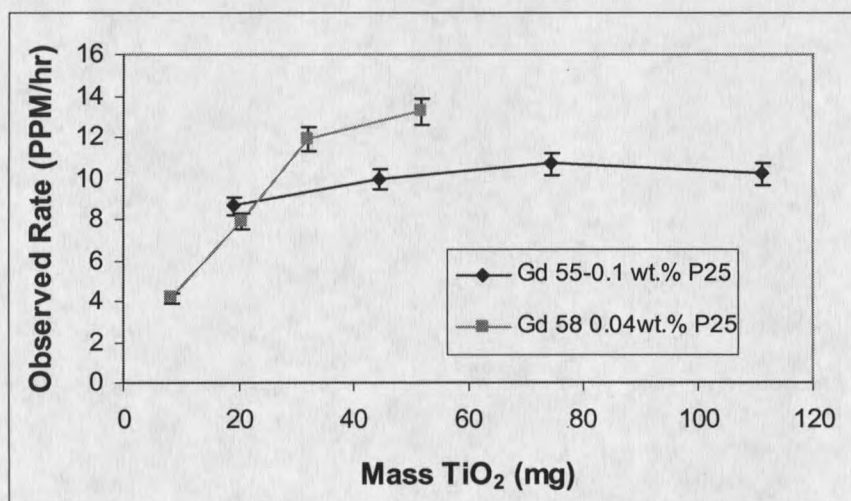


Figure 17. Comparison of Grade 58 and Grade 55 silica gels.

Subsequent light penetration tests conducted on the reactors packed with uncoated Grades 55 and 58 silica (12-18 mesh) showed the two gels to have similar light transmission properties. The difference in intensities between the two gels (Figure 18) is insignificant as there was some variability in measurements due to packing arrangements in the reactors.

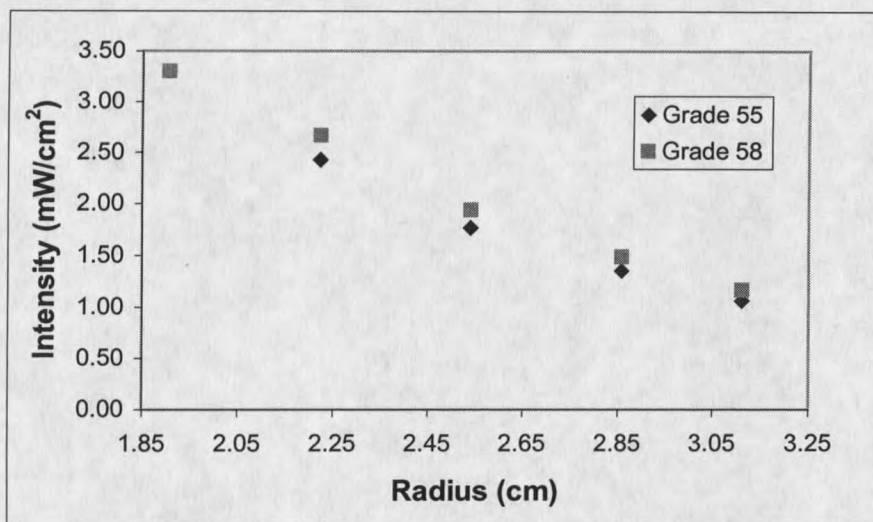


Figure 18. Light penetration tests with uncoated silica gel (12-18 mesh).

To better examine the apparent lower activity of the new silica, a batch of Grade 55 silica with 0.40 weight percent P25 was prepared. This would allow a more direct comparison between the two support materials, weighing its performance against the 0.40 weight percent P25 on Grade 58 silica. With 98 percent of the light absorbed in the smallest reactor with this catalyst, it was expected that no significant increase in rates would be observed in the larger reactors. Runs performed with this catalyst in the largest and smallest reactors confirmed this with little difference in observed degradation rates between the two reactors. However, similar to the 0.1 weight percent loading, rates did not approach the rates attainable with the Grade 58 silica. It is not likely that the difference in activity (nearly 30 % difference in observed rates) can be attributed to a slight increase in light absorption (Figure 18). The lower activity may be related to impurities present in higher quantities in the Grade 55 gel that act to deactivate the

titania. Another possibility is that impurities are present in the Grade 58 silica that enhance the photoactivity of this supported catalyst. Verifying this would require analysis of the silica gels to determine the concentration of any impurities that may be present.

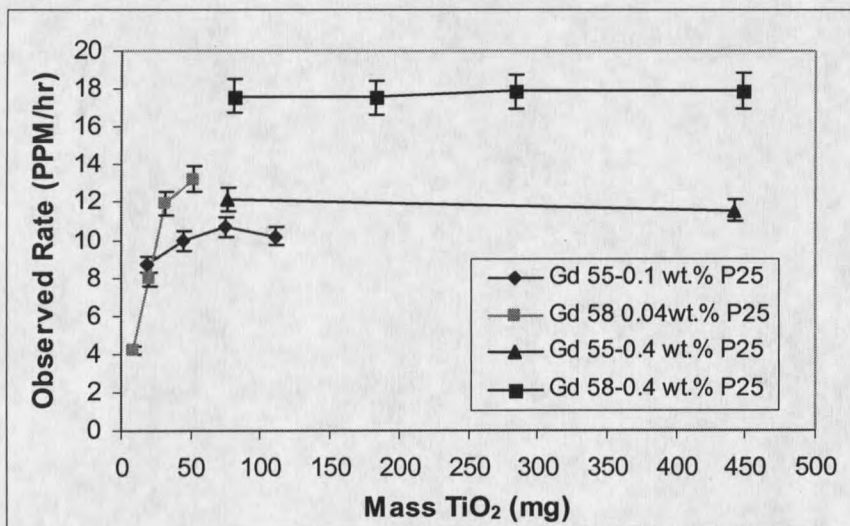


Figure 19. Comparison of observed rates versus mass of titania for the various catalysts.

The rate data for the four catalysts are summarized in Figure 19. Upon comparing the data for the two Grade 58 catalysts, it is apparent that reducing the TiO₂ loading results in decreased catalyst activity. This decrease in activity is likely due to increased absorption of the incident light by the silica gels. It is also apparent that different grades of silica, with similar light transmission properties, will behave quite differently as a support material.

Based on this data, further refinements to the catalysts, with regards to P25 loading, was not attempted. For both grades of silica gel, a 0.40 weight percent loading would appear to be the maximum practical loading for these reactors. Higher loadings

may result in slightly higher rates but would result in unilluminated catalyst in even the smallest reactor.

Slurry Runs

With much of the current research in photocatalysis conducted using TiO_2 slurries, it was desirable to compare the above degradation rates to those obtained with slurries. In reviews of current literature, it was noted that mixed results have been obtained in experiments comparing suspended and supported photocatalysts. Several different researchers (9, 21) have attributed the higher photoactivity of supported titania to increased surface area of the substrate/catalyst and to increased water/organic/oxygen adsorption at the surface. Others (12, 16) have reported better efficiencies using slurries, indicating a higher catalyst surface availability for reactant and photon interactions to be a contributing factor. With the number of variables involved in photocatalysis and the widely varying systems employed, this is not surprising. As much of the work here is preliminary, these experiments were intended to provide a quick comparison between the supported and suspended catalysts in this system and an attempt was not made to extend these findings to other systems.

Slurries were prepared to give total concentrations of P25 in each of the reactors comparable to that for the 0.40 weight percent loaded catalyst. In other words, at any instant during the slurry experiment, the amount of TiO_2 within the annulus would compare to the amount of stationary TiO_2 in the reactor for a 0.40 weight percent loaded silica. At this slurry concentration virtually all of the incoming light was absorbed in the

four reactors and very little or no light was detected at the outer glass once the slurry was introduced.

Runs were conducted in each reactor at the equivalent 0.40 weight percent concentration and one in the largest reactor at double this concentration. The results are presented below in Figure 20.

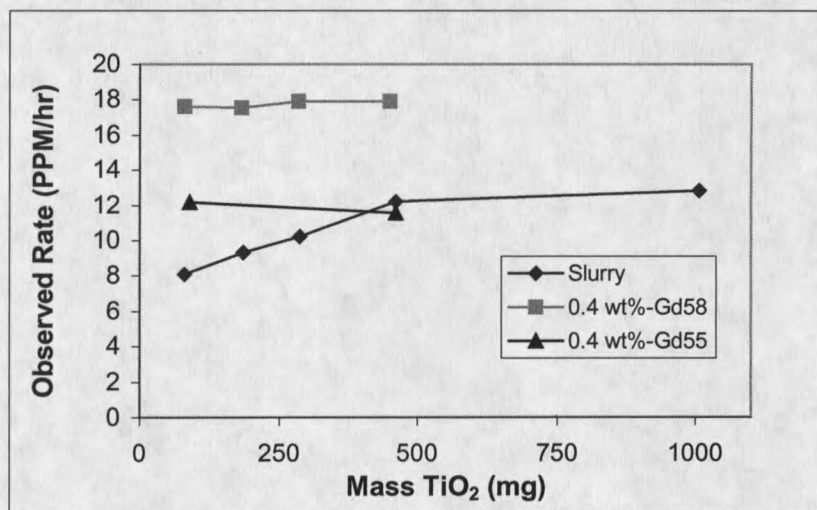


Figure 20. Comparison of observed rates with supported and suspended P25 titania.

Noting that rate increases were observed with increasing reactor diameter, it is probable that light was able to penetrate deeper into the reactors than it was with the packed beds. Though an increase in the rate of degradation was observed with increasing reactor volume, it did not approach rates attainable with the Grade 58 supported catalysts. As it was not feasible to further increase the outer diameter, it was decided to increase slurry concentration in the largest reactor to determine if higher rates were possible. Though changing the concentration of slurry in the reactors changes the depth that light can penetrate, it was reasoned that if rates were significantly higher at a higher slurry

concentration, it would be possible for rates to continue to increase with increasing reactor diameter at the equivalent 0.40 weight percent concentration. More than twice the amount of powder in the largest reactor did little to improve the performance of the slurry. It is evident that sufficient light is not available to increase degradation rates much beyond that attained with the 1210 PPM slurry in the largest reactor. This result correlates well with results presented by Herrmann (4) who found the optimal slurry concentration to be 2500 PPM. Beyond this concentration, rates were determined to be independent of mass of titania.

The fact that higher rates were achieved with Grade 58 supported catalysts in this system does indicate that there are beneficial aspects of immobilizing titania. Whether those benefits are associated with increased adsorption of organics or oxygen remains to be determined and requires further investigation. Another possibility is that the heat treatment of the supported catalysts enhances photoactivity. The powder for the slurries was used as supplied and underwent no refinement. Rate data for the supported and suspended catalyst experiments are summarized in Table 5 below.

Table 5. Summary of supported and suspended observed rates.

Reactor OD (in.)	Degradation Rates (PPM/hr)				Slurry 0.4 Equiv.*
	0.04%P25- Gd58	0.4%P25- Gd58	0.1%P25- Gd55	0.4%P25- Gd55	
2.00	4.1	17.6	8.7	12.2	8.1 (780 PPM TiO ₂)
2.25	7.9	17.5	10	---	9.3 (1020 PPM TiO ₂)
2.50	11.9	17.9	10.7	---	10.2 (1060 PPM TiO ₂)
2.75	13.2	17.9	10.2	11.5	12.2 (1210 PPM TiO ₂) 12.8 (2650 PPM TiO ₂)

*Plus one run in largest reactor at more than twice this concentration

Data Analysis

Due to the nature of photocatalytic systems, rate constants will be a function of several external parameters such as light intensity, catalyst loading, support material, and catalyst preparation methods. With the variety of experimental conditions used by current research groups, a significant comparison of data becomes difficult. Consideration was given to factor out some parameters in this project. All runs were performed at the same flow rate, initial substrate concentration, initial light intensity (i.e. same light used in each reactor), and make of titanium dioxide. The inadvertent use of different support materials in these experiments further complicated internal comparisons. To better correlate the data, an attempt was made to compare rate constants based on the rate of light absorption in each reactor.

Volume Correction

It was noted above that formic acid degradation follows apparent zero order kinetics at higher concentrations. Referring to the experimental setup used, rate constants were calculated using the concentration-time history in the tank. The setup used is essentially a constant volume batch system consisting of a plug flow photoreactor (PFR) in a recirculation loop and a well stirred, nonreacting mixing tank. The formic acid solution is degraded only while under illumination in the reactor and is returned to the tank where it dilutes the bulk solution. Small differential conversions were obtained with each pass through these photoreactors (generally less than 1 %).

